https://doi.org/10.30799/jnst.S205.26110305 J. Nanosci. Tech. - Volume 11 Issue 3 (2026) 1093–1095

Share Your Innovations through JACS Directory

Journal of Nanoscience and Technology

Visit Journal at https://www.jacsdirectory.com/jnst

ISSN: 2455-0191

Synthesis and Characterizations of CeO_2 Nanoparticles for Gas Sensing Application

Maheshwari B. Suryawanshi*, Gokul V. Suryawanshi, Tulshidas S. Savale

Department of Chemistry, M.G.V's M.S.G. Arts, Science and Commerce College, Malegaon Camp, Malegaon, Nashik – 423 105, Maharashtra, India.

ARTICLEDETAILS

Article history:
Received 24 February 2026
Accepted 11 March 2026
Available online 15 April 2026

Keywords:
Cerium(IV) Oxide Nanoparticles
Co-Precipitation
Gas Sensor
Nanocrystal

ABSTRACT

Cerium oxide (ceria, CeO_2) nanoparticles were successfully synthesized in the present work using the co-precipitation (CPT) method with potassium carbonate and cerium tri-nitrate hexahydrate as precursor solutions. The preparation involved controlled precipitation followed by aging and thermal treatment to enhance crystallinity. The obtained powder was then gently ground and calcined at two different temperatures, 700 °C and 850 °C, for three hours each to examine the effect of thermal treatment on structural, vibrational, and morphological properties. A set of analytical techniques, including X-ray diffraction (XRD), energy dispersive X-ray spectroscopy (EDS), and field-emission scanning electron microscopy (FE-SEM), were employed to evaluate the crystalline phase formation, chemical composition, and microstructural characteristics of the ceria NPs. XRD analysis confirmed that the synthesized samples crystallize in a single-phase cubic fluorite structure without any secondary phases or impurities. The calculated lattice parameters were 5.392 Å for the sample calcined at 700 °C and 5.357 Å for the sample calcined at 850 °C, demonstrating a slight reduction in lattice parameter with increasing calcination temperature. Chemical composition analysis via EDS verified the presence of cerium (Ce) and oxygen (O), thereby confirming the successful formation of CeO_2 without contamination. FE-SEM micrographs revealed that the ceria NPs exhibit a predominantly spherical morphology with uniform size distribution. Mild agglomeration was observed, which is typical for nanoparticles due to high surface energy and interparticle attractive forces. The crystalline, high-purity Ceria NPs produced in this work possess desirable structural and morphological attributes that make them promising candidates for advanced functional applications including catalysis, fuel cells, optical devices, and environmental remediation.

1. Introduction

Cerium oxide (CeO_2) nanoparticles have attracted considerable attention due to their outstanding physicochemical properties and broad technological applications [1]. As a versatile rare-earth oxide, ceria is widely employed in catalysis, photochemistry, electrochemistry, materials science, biomedical fields, and luminescent technologies [2]. It serves as an efficient oxidation catalyst, a strong ultraviolet (UV) absorber, and a counter electrode material in solid oxide fuel cells (SOFCs), electrochemical devices, and LPG sensors [3]. The remarkable functionality of CeO_2 arises from its ability to reversibly switch between Ce^{4+} and Ce^{3+} oxidation states [4,5]. Cerium, with the electronic configuration $4f^15d^16s^2$, exhibits mixed valence behaviour that contributes to its semiconducting properties and high oxygen storage capacity [6]. Structurally, CeO_2 crystallizes in a cubic fluorite lattice (space group Fm3m), where each Ce^{4+} ion is coordinated by eight O^{2-} ions in a symmetrical arrangement [7]. The reversible redox transition between Ce^{4+} and Ce^{3+} facilitates the formation and migration of oxygen vacancies, which strongly influence its catalytic, electrical, and optical properties [8]. These oxygen vacancies introduce localized lattice distortions and generate intrinsic defects, while extrinsic defects may arise from dopants or synthesis-related impurities [9,10]. Such point defects significantly affect ionic conductivity, luminescence, and diffusion behaviour [11]. At elevated temperatures (above 650°C), partial reduction of Ce^{4+} to Ce^{3+} occurs, accompanied by the formation of oxygen vacancies, enhancing the redox capacity and suitability of ceria for high-temperature applications [12]. Various synthesis techniques including sol–gel, hydrothermal, forced hydrolysis, spray pyrolysis, and co-precipitation—have been developed to control particle size, crystallinity, and defect concentration [13]. However, achieving uniformly small particles with narrow size distribution remains challenging, especially when high-temperature calcination is required for improved crystallinity [14].

In this study, cerium oxide nanoparticles are synthesized via the co-precipitation method, a simple and cost-effective approach, and calcined at 700 °C and 850 °C to investigate their structural, morphological, and particle size characteristics.

2. Experimental Methods

2.1 Synthesis of CeO_2 NPS

Cerium oxide (CeO_2) nanoparticles were synthesized by a co-precipitation method using cerium nitrate hexahydrate [$Ce(NO_3)_3{\cdot}6H_2O$] and potassium carbonate (K_2CO_3) as precursor and precipitating agent, respectively. A 0.1 M cerium nitrate solution (4.34 g in 100 mL deionized water) was prepared under magnetic stirring at 500 rpm. A 0.1 M K_2CO_3 solution was added dropwise (~1 mL/min) until the pH reached 9–10, resulting in the formation of a cerium carbonate precipitate. The mixture was stirred for 2 h and aged for 12 h for complete precipitation. The precipitate was filtered, washed with deionized water and ethanol to remove residual ions, and dried at 80 °C for 6 h. Finally, the dried precursor was calcined at 600 °C for 3 h to obtain crystalline CeO_2 nanoparticles. Calcination enhanced crystallinity and oxygen vacancy formation, improving redox behaviour and gas-sensing properties.

3. Results and Discussion

3.1 UV–Visible Analysis

The UV–Visible absorption spectrum of the synthesized pure CeO_2 sample exhibits a strong and broad absorption band in the ultraviolet region, characteristic of charge-transfer transitions from $O^{2-} \rightarrow Ce^{4+}$ within the CeO_2 lattice (Fig. 1). The spectrum shows a maximum absorbance in the range of approximately 250–280 nm, followed by a gradual decline as the wavelength increases. A sharp decrease in absorption is observed near 350–380 nm, indicating the optical absorption edge of the material. Using this absorption edge, the optical

*Corresponding Author:mayusurya2004@gmail.com(M.B. Suryawanshi)

https://doi.org/10.30799/jnst.S205.26110305

band gap was estimated to be around 3.4–3.5 eV, which falls within the expected range for nanocrystalline CeO_2 and confirms its semiconductor nature. The absence of additional absorption peaks in the visible region suggests good phase purity, with no detectable impurity-related electronic transitions. The strong UV absorption and wide band gap further confirm the suitability of the synthesized CeO_2 nanoparticles for applications such as UV shielding, photocatalysis, and optoelectronic devices. Overall, the UV–Visible analysis indicates that the material possesses high optical activity in the UV region, stable semiconductor behaviour, and a band structure favourable for light-driven surface reactions.

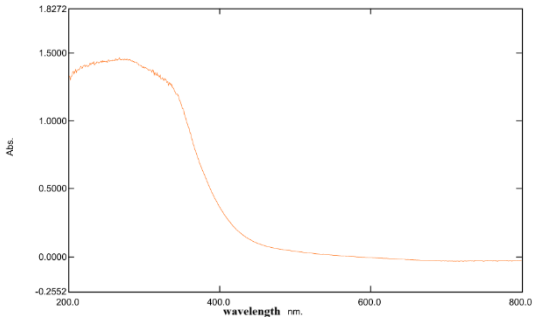

Fig. 1 UV–visible absorption spectrum of synthesized CeO_2 nanoparticles

3.2 FE-SEM Analysis

The FE-SEM micrographs confirm that the synthesized material exhibits a distinctly nanostructured morphology composed of irregularly shaped and highly agglomerated nanoparticles forming a porous, interconnected network (Fig. 2). The particle size distribution varies noticeably across the samples, with the first micrograph showing the smallest crystallites in the range of approximately 10–28 nm, indicative of fine nanoscale particle formation. The second and third images display progressively larger nanoparticles, ranging from 40–86 nm and 50–70 nm, respectively, reflecting increased particle growth and aggregation during synthesis or subsequent thermal treatment. The fourth micrograph reveals a densely packed structure with severe agglomeration, where individual particles are no longer distinguishable, suggesting extensive grain coalescence. This gradation in particle size and agglomeration behaviour highlights the influence of synthesis parameters on morphological evolution. Overall, the FE-SEM analysis demonstrates that the material possesses a high degree of porosity and strong agglomeration tendency, characteristics that are advantageous for applications requiring enhanced surface area and active sites, such as photocatalysis, gas sensing, adsorption, and electrochemical processes.

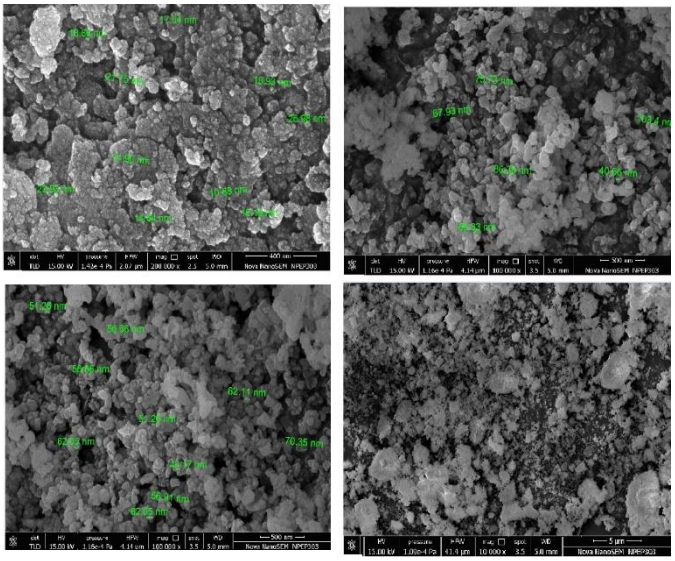

Fig. 2 SEM micrographs of synthesized CeO_2 nanoparticles

3.3 EDS Analysis

The EDS spectrum of the synthesized CeO_2 sample confirms the elemental composition and purity of the material. Distinct and well-defined peaks corresponding to cerium (Ce) and oxygen (O) are clearly observed, with no additional impurity peaks detected in the scanned energy range (Fig. 3) The elemental composition and purity of the synthesized CeO_2 nanoparticles were confirmed by EDS analysis. The strong oxygen peak around ~0.5 keV and multiple characteristic Ce peaks between ~0.8–5.5 keV (including Ce M and Ce L lines) verify the successful formation of cerium oxide. The absence of any foreign elements indicates high chemical purity and confirms that no unintended metallic or non-metallic contaminants were introduced during synthesis. The relative intensities of the Ce and O peaks further support the stoichiometric presence of cerium and oxygen, consistent with the expected CeO_2 phase. Overall, the EDS analysis validates that the synthesized nanoparticles are compositionally pure cerium oxide, complementing the structural and morphological findings obtained from UV–Visible and FE-SEM characterizations.

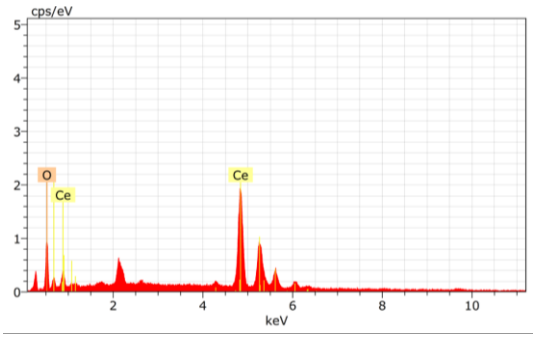

Fig. 3 EDX spectrum of synthesized CeO_2 nanoparticles

3.4 FT-IR Analysis

The FTIR spectrum of the synthesized sample reveals several characteristic vibrational bands confirming the formation of metal–oxygen bonds along with the presence of surface functional groups typically associated with cerium oxide nanoparticles (Fig. 4). A broad and intense absorption band centered around ~3392 cm^{-1} corresponds to O–H stretching vibrations, indicating the presence of adsorbed moisture and surface hydroxyl groups, which are commonly retained on CeO_2 surfaces due to their high affinity for water molecules. The weak features near ~2842 cm^{-1} may be attributed to C–H stretching vibrations arising from trace organic residues or atmospheric contamination. A distinct absorption peak observed near ~1632 cm^{-1} is assigned to the bending mode of molecularly adsorbed water (H–O–H), further supporting surface hydration of the nanoparticles. Multiple peaks in the region between 1200–600 cm^{-1} correspond to various metal–oxygen lattice vibrations. In particular, the strong bands appearing near ~622, ~558, and ~523 cm^{-1} are characteristic of Ce–O and Ce–O–Ce stretching modes, confirming the successful formation of cerium oxide. The absence of additional significant peaks suggests high purity of the synthesized CeO_2, with no major organic or inorganic impurities present. Overall, the FTIR analysis validates the presence of Ce–O bonding, surface hydroxylation, and structural integrity of the synthesized metal oxide nanoparticles.

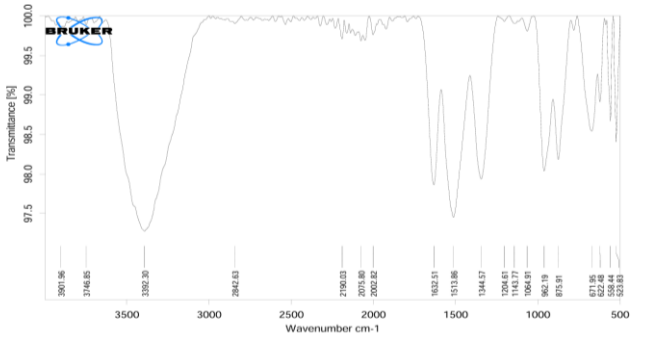

Fig. 4 FTIR spectrum of synthesized CeO_2 nanoparticles

3.5 XRD Analysis

The XRD pattern of the synthesized sample displays a series of sharp and intense diffraction peaks, confirming the formation of a well-crystallized crystalline phase (Fig. 5). The crystalline structure of CeO_2 nanoparticles is confirmed by the XRD pattern prominent reflections appearing at 2θ values around ~28.5°, 33.1°, 47.5°, 56.3°, 59.1°, 69.4°, and 77.1° correspond to the (111), (200), (220), (311), (222), (400), and (331) planes, respectively. These reflections match well with the standard cubic fluorite structure of CeO_2 (JCPDS No. 34-0394), verifying that the synthesized material possesses a pure single-phase cerium oxide crystalline framework. The absence of any additional impurity peaks indicates high phase purity, with no detectable traces of secondary oxides or other crystalline impurities. The strong intensity of the (111) reflection

https://doi.org/10.30799/jnst.S205.26110305

Cite this Article as: Maheshwari B. Suryawanshi, Gokul V. Suryawanshi, Tulshidas S. Savale, Synthesis and characterizations of CeO_2 nanoparticles for gas sensing application, J. Nanosci. Tech. 11(3) (2026) 1093–1095.

suggests that this plane is the preferred orientation during the material's growth process. The moderate broadening of the peaks is indicative of nanoscale crystallite formation, which aligns well with the FESEM observations. Estimation of crystallite size 30 nm using the Debye–Scherrer equation confirms the nanoscale nature of the CeO_2 crystallites. Overall, the XRD analysis conclusively demonstrates the formation of highly crystalline, phase-pure cubic CeO_2 nanoparticles with nanoscale crystallite dimensions, reinforcing the structural integrity and successful synthesis of the material.

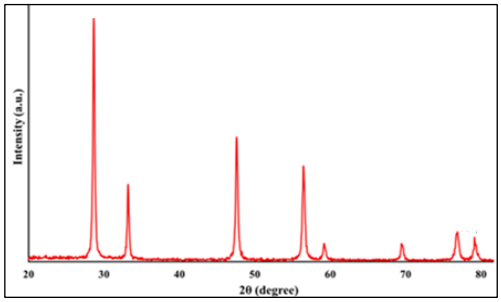

Fig. 5 X-ray diffraction (XRD) pattern of synthesized CeO_2 nanoparticles

3.6 Gas Sensing Results

The gas-sensing characteristics of CeO_2 nanoparticles reveal a strong temperature-dependent response toward LPG, methanol, ethanol, and NH_3, with sensitivity increasing from 40 °C up to an optimum of around 160 °C, after which it decreases due to reduced surface oxygen adsorption at higher temperatures (Fig. 6a). The temperature-dependent gas sensing response of CeO_2 nanoparticles is illustrated LPG exhibits the highest sensitivity (reaching ~60%) because the Ce^{4+}/Ce^{3+} redox mechanism and abundant oxygen vacancies promote effective chemisorption and rapid electron exchange between LPG molecules and the CeO_2 surface (Fig. 6b)

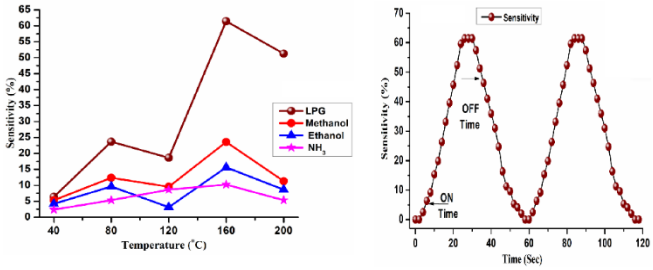

Fig. 6 a) Variation of gas sensitivity (%) of CeO_2–ZnO nanocomposite sensor toward gases as a function of operating temperature (40–200 °C); and b) Dynamic response–recovery characteristics of the CeO_2–ZnO gas sensor showing sensitivity variation with time and indicating ON and OFF response cycles

The response–recovery behaviour and repeatability of the sensor are presented methanol and ethanol show moderate sensitivities because their molecular structures enable interaction with surface oxygen species, yet their adsorption energies and reaction kinetics are lower compared to LPG. NH_3 shows the weakest response due to its lower affinity toward CeO_2 and faster desorption rate at elevated temperatures. The dynamic response–recovery study further demonstrates that CeO_2 possesses excellent switching behaviour, with a sharp rise in sensitivity immediately after gas exposure (ON time) and a quick return to baseline once the gas is removed (OFF time), confirming efficient oxygen re-adsorption and surface regeneration. The repeated cycling pattern indicates highly stable operation, good reproducibility, and minimal degradation over time. Overall, the results underline that CeO_2 nanoparticles offer high gas-sensing performance with rapid and reversible response–recovery characteristics, strong selectivity toward LPG, and optimal operation at 160 °C, making them promising candidates for reliable, real-time gas detection and safety monitoring applications.

4. Conclusion

Ceria (CeO_2) nanoparticles were successfully synthesized via a co-precipitation method under optimized reaction conditions to obtain high-purity nanocrystalline powder. Controlled precipitation of cerium ions ensured uniform nucleation, while subsequent washing, drying, and calcination promoted the formation of well-defined crystalline particles. X-ray diffraction (XRD) analysis confirmed the formation of a single-phase cubic fluorite structure without any secondary phases, indicating the effectiveness of the synthesis route. The calculated average crystallite size ranged from 11.3 to 15.6 nm, demonstrating controlled nanoscale growth. Morphological characterization using FE-SEM revealed nearly spherical nanoparticles with slight agglomeration due to high surface energy. The particles were uniformly distributed, forming a porous and interconnected structure advantageous for catalytic and gas-sensing applications. Energy-dispersive X-ray spectroscopy (EDX/EDS) confirmed the elemental purity of the material, showing only cerium and oxygen peaks consistent with stoichiometric CeO_2.

FTIR spectra exhibited characteristic Ce–O and Ce–O–Ce vibrational modes along with surface hydroxyl groups. UV–Visible analysis showed strong absorption in the UV region with an absorption edge around 350–380 nm and an estimated band gap of ~3.4–3.5 eV, confirming semiconducting behaviour. The co-precipitation method proved to be a simple, economical, and efficient approach for producing phase-pure CeO_2 nanoparticles with controlled size and desirable morphology. The presence of oxygen vacancies and nanoscale dimensions enhances surface reactivity and adsorption capacity. Gas-sensing studies demonstrated strong sensitivity, particularly toward H_2S gas, indicating the potential of the synthesized CeO_2 nanoparticles for sensor, catalytic, and environmental applications.

References

[1] S. Pansambal, R. Oza, S. Borgave, A. Chauhan, P. Bardapurkar, S. Vyas, S. Ghotekar, Bioengineered cerium oxide (CeO_2) nanoparticles and their diverse applications: a review, Appl. Nanosci. 13(9) (2023) 6067–6092.

[2] L. He, Y. Su, S. Shi, Recent advances of cerium oxide nanoparticles in synthesis, luminescence and biomedical studies: a review, J. Rare Earths 33(6) (2015) 791–799.

[3] A. Talukdar, A. Chakrovorty, P. Sarmah, P. Paramasivam, V. Kumar, S.K. Yadav, S. Manickkam, A review on solid oxide fuel cell technology: an efficient energy conversion system, Int. J. Energy Res. 2024 (2024) 6443247.

[4] V. Seminko, P. Maksimchuk, Cerium oxide nanocrystals (CeO_2–x): Defects, luminescence and redox activity, Springer Nature, USA, 2026.

[5] S. Kumar, P.C. Arya, C. Mondal, A. Sinha, Rare-earth doped ceria: comparative insights into synthesis, defect engineering, and functional applications, Ionics 32 (2026) 1–28.

[6] K. Mužina, I.K. Ivković, S. Kurajica, Electrochemical and catalytic applications of cerium (IV) oxide, Eng. Power Bull. Croat. Acad. Eng. 17 (2022) 6–13.

[7] S. Boskovic, B. Matovic, M. Van Asten, Nanostructured solid solutions of the fluorite type crystal structure, in: Fluorite, Structure, Chemistry and Application, Nova Science Publishers, New York, 2019, pp.1-111.

[8] M.E. Khan, M.M. Khan, M.H. Cho, Ce^{3+}-ion, surface oxygen vacancy, and visible light-induced photocatalytic dye degradation and photocapacitive performance of CeO_2-graphene nanostructures, Sci. Rep. 7 (2017) 5928.

[9] B. Bhagvat, R.S. Gupta, P. Patel, S.K. Sahoo, A. Rahaman, et al., Unravelling defect mediated magnetism in anatase TiO_2 nanoparticles through structural, optical, and magnetic characterizations, J. Supercond. Nov. Magn. 38 (2025) 25.

[10] J. Zhong, A.H. Kitai, P. Mascher, W. Puff, The influence of processing conditions on point defects and luminescence centers in ZnO, J. Electrochem. Soc. 140(12) (1993) 3644–3649.

[11] C. Zhang, J. Lin, Defect-related luminescent materials: synthesis, emission properties and applications, Chem. Soc. Rev. 41 (2012) 7938–7961.

[12] S.G. Peera, S.W. Kim, Rare earth Ce/CeO_2 electrocatalysts: role of high electronic spin state of Ce and Ce^{3+}/Ce^{4+} redox couple on oxygen reduction reaction, Nanomaterials 15 (2025) 600.

[13] J. Leng, Z. Wang, J. Wang, H.H. Wu, G. Yan, et al., Advances in nanostructures fabricated via spray pyrolysis and their applications in energy storage and conversion, Chem. Soc. Rev. 48 (2019) 3015–3072.

[14] Y. Han, Y. Lei, J. Ni, Y. Zhang, Z. Geng, et al., Q. Xiao, Single-crystalline cathodes for advanced Li-ion batteries: progress and challenges, Small 18(21) (2022) 2107048.

https://doi.org/10.30799/jnst.S205.26110305

Cite this Article as: Maheshwari B. Suryawanshi, Gokul V. Suryawanshi, Tulshidas S. Savale, Synthesis and characterizations of CeO_2 nanoparticles for gas sensing application, J. Nanosci. Tech. 11(3) (2026) 1093–1095.